JQS Journal of Quaternary Science

QRA
Quaternary Research Association

Late Devensian deglaciation of south-west Wales from luminescence and cosmogenic isotope dating

N. F. GLASSER,[1]* J. R. DAVIES,[1] M. J. HAMBREY,[1] B. J. DAVIES,[2] D. M. GHEORGHIU,[3] J. BALFOUR,[1] R. K. SMEDLEY[4] and G. A. T. DULLER[1]
[1]Department of Geography and Earth Sciences, Aberystwyth University, UK
[2]Department of Geography, Royal Holloway University of London, UK
[3]Scottish Universities Environmental Research Centre, East Kilbride, UK
[4]Department of Geography and Planning, University of Liverpool, UK

ABSTRACT: The Welsh Ice Cap was a dynamic component of the last British–Irish Ice Sheet at the Last Glacial Maximum, but there are few chronological constraints on the pace and timing of deglaciation. This paper presents new geomorphological and geochronological evidence that constrains the timing of the separation of the Welsh Ice Cap from the Irish Sea Ice Stream and the subsequent deglaciation of south-west Wales; and allow these to be assessed in the context of late Pleistocene climatic events. Luminescence ages from glacial outwash sediments south of Cardigan demonstrate that the Irish Sea Ice Stream was receding by ∼26.7 ka. The subsequent recession of the Welsh Ice Cap is documented by cosmogenic ages from landforms and sediments in the Aeron and Teifi valleys and upland areas. Deglaciation of the Cambrian Mountains was underway by ∼19.6 ka. Cross-valley moraines and associated deglaciation deposits show that minor re-advances interrupted the recession of the Aeron Glacier twice, and the Teifi Glacier on at least 12 occasions. By ∼14.9 ka, the Aeron valley was probably ice-free, but the northwards withdrawal of the Teifi glacier had halted in the Tregaron area. The final rapid recession of this glacier into the uplands of central Wales was completed during the Windermere Interstadial (13.5 cal ka BP) when, in common with much of the UK, the whole of Wales is believed to have become ice-free. There is no evidence that the Cambrian Mountains contained ice-free enclaves at the Last Glacial Maximum, as has been previously suggested. The new ages presented here support suggestions that there was rapid change in the configuration of the Welsh Ice Cap between 20 and 17 ka as upland areas became exposed and there was increasing topographic control on patterns of ice discharge. © 2018 The Authors. *Journal of Quaternary Science* Published by John Wiley & Sons Ltd.

KEYWORDS: cosmogenic isotopes; deglaciation; Irish Sea Ice Stream; luminescence dating; Welsh Ice Cap.

Introduction

Both modelling studies and observations show that the last British–Irish Ice Sheet (BIIS) was a dynamic and rapidly changing ice mass (Hubbard *et al.*, 2009; Chiverrell *et al.*, 2013; Patton *et al.*, 2013a,b,c; Clark *et al.*, 2018). Scourse *et al.* (2009) also interpreted dynamism, and rapid response to millennial-scale forcing, in their analysis of the continuous ice-rafted detritus record from the adjacent deep sea. This dynamism was largely due to its relatively small size, which was constrained by the continental shelf break, and proximity to the warm North Atlantic Current, part of the Atlantic Meridional Overturning Circulation (Clark *et al.*, 2012). Early numerical simulations of the BIIS (e.g. Boulton *et al.*, 1977, 1985, 1991; Lambeck, 1993, 1995) suggested that it was an uncomplicated feature, largely centred over the Scottish Highlands, and with gradually decreasing ice-surface elevation across the rest of the country. However, this view differs from that derived from empirical geomorphological and geochronological evidence, which indicates that at the Last Glacial Maximum (LGM), the BIIS was composed of several small, semi-independent ice caps or ice-dispersal centres (McCarroll and Ballantyne, 2000; Golledge *et al.*, 2008; Hubbard *et al.*, 2009; Hughes *et al.*, 2014; Figure 1). The Welsh Ice Cap was one such centre and the timing of recession of this and other sectors of the BIIS are also debated (e.g. Ballantyne, 2010; Chiverrell *et al.*, 2013; Everest *et al.*,

2013; Hughes *et al.*, 2011). We use here the global LGM definition of Peltier and Fairbanks (2006), which places it around 26 ka.

Several workers have attempted to develop a chronology for recession of the Irish Sea Ice Stream and the Welsh Ice Cap (e.g. Ballantyne, 2010; Chiverrell *et al.*, 2013; Patton *et al.*, 2013a,b), but uncertainties remain. Initial work using cosmogenic nuclide ages along the coast implied that decoupling of the two ice masses and deglaciation of the southern Irish Sea Basin was well underway by 23–22 ka (McCarroll *et al.*, 2010) despite some age estimates of 33–100 ka being obtained (Ballantyne, 2010). Although the geomorphology of the landscape produced by the Welsh Ice Cap is reasonably well documented (e.g. Etienne *et al.*, 2005; Jansson and Glasser, 2005), little is known about its recessional history. Recent geochronology in Snowdonia (Glasser *et al.*, 2012; Hughes *et al.*, 2016; Figure 2A) corroborates modelling simulations (e.g. Patton *et al.*, 2013a,b) that show a previously extensive ice cover evolving into a series of valley glaciers. These individual glaciers receded progressively up-valley into accumulation areas in the Cambrian Mountains and Snowdonia. Significantly, the new exposure ages from Snowdonia point to a rapid change in ice-mass configuration between 20 and 17 ka accompanied by transition from an ice cap to a thinning highland ice field with nunataks (Hughes *et al.*, 2016). Before the current study, this apparent rapid change had not been revealed elsewhere in Wales, leaving questions about rates of deglaciation and deglacial dynamics of the Welsh sector of the BIIS.

*Correspondence: Neil Glasser, as above.
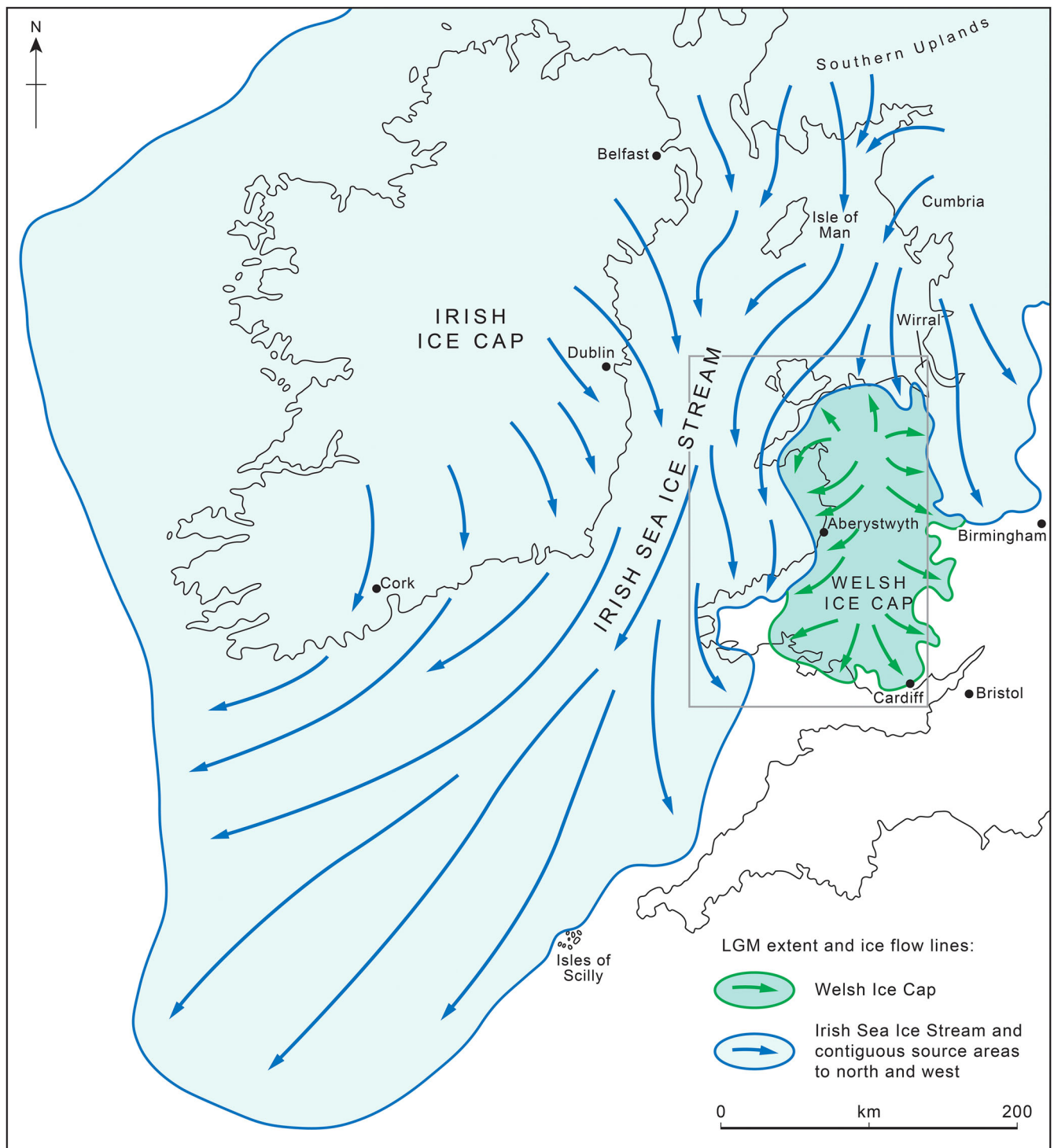E-mail: nfg@aber.ac.uk

Figure 1. Overview of the last British–Irish Ice Sheet at the Last Glacial Maximum (modified from Hambrey *et al.*, 2001 and Jenkins *et al.*, 2018). Note the ice source regions over Ireland, the Southern Uplands of Scotland and northern England, which contributed to the Irish Sea Ice Stream. The location of the Welsh Ice Cap is also shown. Inset box shows location of Fig. 2. [Colour figure can be viewed at wileyonlinelibrary.com]

Clark *et al.* (2012, 2018) and Hughes *et al.* (2011, 2014) provided comprehensive reviews of the geochronological evidence for the glaciation in the British Isles and concluded that the BIIS reached its maximum extent at different times in different sectors. In many parts of Britain, Ireland and the North Sea, ice had reached its maximum extent by 27 ka. For example, the earliest maximum advances recognized by Clark *et al.* (2012) occurred by 27 ka in the North Sea and off the coast of NW Scotland. More recently, the maximum southern extent of the Irish Sea Ice Stream on the Isles of Scilly has been dated to 26–25 ka (Smedley *et al.*, 2017a). According to Chiverrell *et al.* (2013), the maximum extent of

Devensian ice was delayed until 25.3 and 24.5 ka near our study area in Wales. A large-scale review by Ballantyne (2010) also suggests a glacial maximum in this area between 26 and 21 ka.

During the early stages of the Devensian Glaciation, the Welsh Ice Cap developed as a separate and autonomous feature and the mountainous areas of North Wales provide constraints on ice-surface elevation (Glasser *et al.*, 2012; Hughes *et al.*, 2016). Most evidence points to the Snowdon massif as a major centre of ice dispersal, with either small domes situated above satellite massifs or a continuous ice divide running broadly north to south (Jansson and Glasser,

2005) (Fig. 1). The thickest part of the ice cap was positioned over the Arenig and Aran mountains (Fearnsides, 1905; see Fig. 2 for locations named in the text), with ice flowing westwards from these areas towards Cardigan Bay (Foster, 1970a,b) and eastwards towards the border with England (Travis, 1944). To the north and west, the ice cap interacted and coalesced with a southwards-moving ice mass sourced from northern sectors of the BIIS, which occupied the site of the current Irish Sea Basin (Fig. 1). The distinctive deposits of this Irish Sea Ice Stream mark its maximum extent (McCarroll et al., 2010; Chiverrell et al., 2013).

Where it was unimpeded, the Irish Sea Ice Stream spread across the Cheshire Plain into north-east Wales, the northern Vale of Clwyd (Rowlands, 1971; Thomas, 1985, 1989; Davies et al., 2004), Anglesey and the Llŷn Peninsula (Thomas and Chiverrell, 2007) as part of its southwards progress into Cardigan Bay and across the coastal tract of south-west Wales (Fig. 1). In all these areas, the landward advance of Irish Sea ice was halted by the expanding Welsh Ice Cap so that at the time of the LGM a complex interface existed between the two competing ice masses. The deposits and landforms that locate this zone of interaction have been identified in north Wales (Thomas, 1989; Davies et al., 2004) and in south-west Wales (Davies et al., 2006b). The southward progress of the Irish Sea Ice Stream into south-west Wales was halted locally by the uplands of the Preseli Mountains, which it failed to overtop even at the time of the LGM (Burt et al., 2012). The large ice-dammed glacial Llyn (Lake) Teifi, once thought to have formed during ice recession (e.g. Charlesworth, 1929;

Jones, 1965), is now known to have developed between the two converging ice masses during their Late Devensian advance into the Teifi Valley (Waters et al., 1997; Fletcher and Siddle, 1998; Hambrey et al., 2001; Etienne et al., 2006).

Here we present new luminescence and cosmogenic isotope (surface exposure) ages obtained for the coastal tract and river catchments of south-west Wales and the southern Cambrian Mountains. These new ages, when interpreted in the context of associated glacial landforms and deposits, provide insight into the post-LGM behaviour of the Welsh Ice Cap, notably its separation from the Irish Sea Ice Stream, and subsequent history and pattern of deglaciation.

Study area: geology and geomorphology

This paper focuses on the Teifi, Aeron and Ystwyth river catchments and the flanking upland regions of the southern Cambrian Mountains and Mynydd Bach (Fig. 2). This region was covered by the Welsh Ice Cap and its confluence with the south-eastern margin of the Irish Sea Ice Stream (Fig. 1). South of the Ystwyth valley, the deeply dissected Cambrian Mountains plateau widely achieves elevations above 450 m with a maximum elevation near the headwaters of the Teifi of 594 m. The more westerly Mynydd Bach plateau, on which the River Aeron rises, and which widely exceeds 300 m in elevation, overlooks the lower ground that forms the Cardigan Bay coastal tract. In the far south of the study area, the prominent rock tors of the Preseli Mountains rise to elevations over 460 m. The bedrock of the area principally comprises
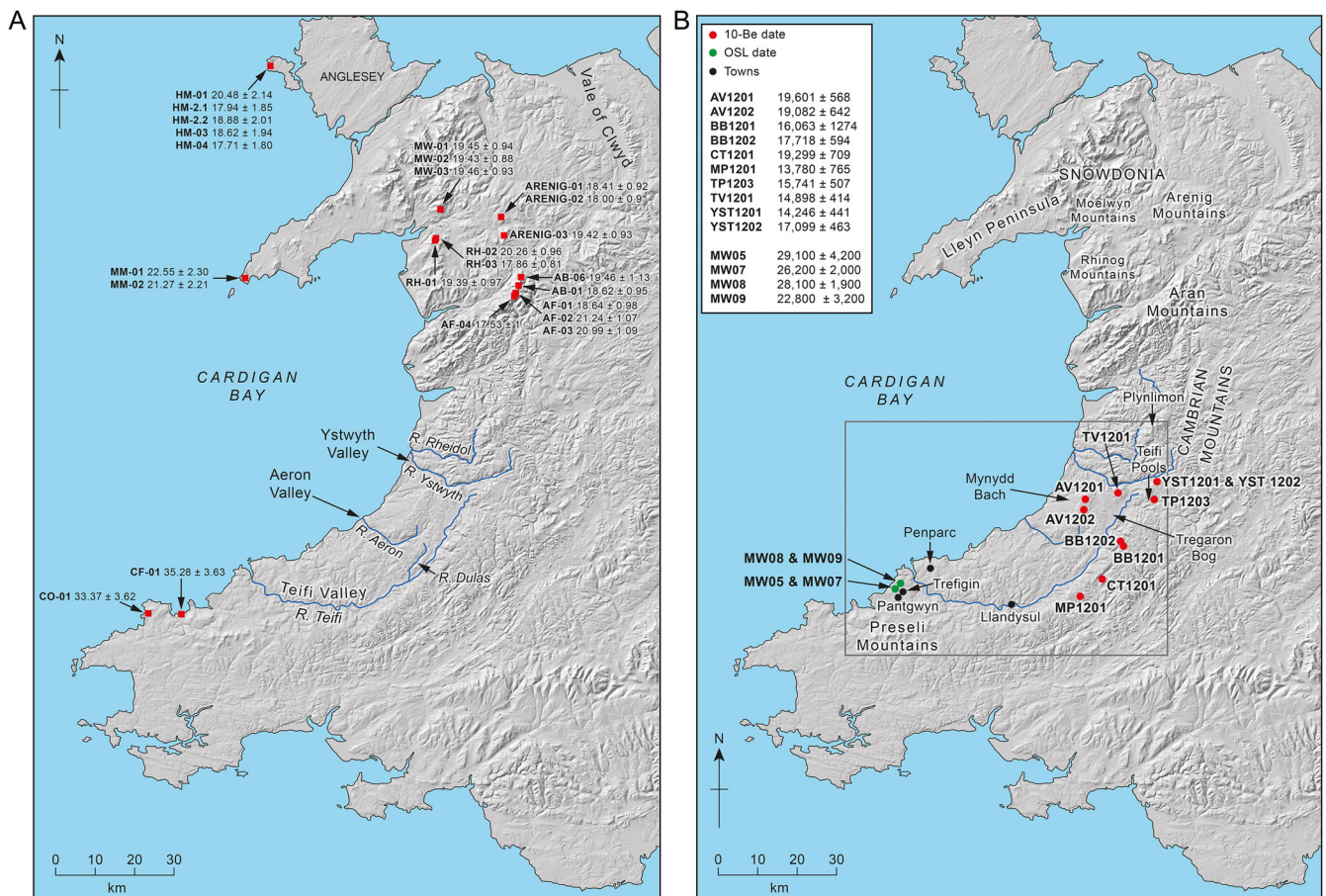

Figure 2. A. Published cosmogenic isotope ages dates relating to deglaciation events in Wales (Phillips et al., 1994; McCarroll et al., 2010; Glasser et al., 2012; Hughes et al., 2016). Note that four samples referred to in Phillips et al. (1994) are not induced here because no detailed site information is provided that allows us to plot their locations accurately. B. Map of Wales indicating place names mentioned in the text and samples dated in this study. The Teifi, Aeron and Ystwyth valleys are indicated. Background is a hill-shaded NEXTMap DEM provided by Intermap Technologies. Inset box shows location of Fig. 6. [Colour figure can be viewed at wileyonlinelibrary.com]

interbedded mudstone, sandstone and localized conglomer-
ate deposited by turbidity currents and other mass-flow
processes. Most are of Silurian age, but Ordovician rocks that
also include volcanic and intrusive igneous units occur in the
south and west (e.g. Davies *et al.*, 1997, 2006a,b; Burt *et al.*,
2012). NE–SW-trending bedrock lineaments reflect the domi-
nant geological structural trend imposed by late Caledonian
orogenesis (e.g. Davies *et al.*, 1997). However, the modern
drainage systems only locally reflect this structural grain
with major ENE–WSW-trending cross faults also influential.
Before the Cenozoic capture of its headwaters by the rivers
Rheidol and Ystwyth the source of the previously much larger
River Teifi was located on the flanks of the Plynlimon
(Pumlumon) Dome. Broad glaciated hollows indicate
the abandoned former course of this palaeo-River Teifi in
the north of the study area. Waters *et al.* (1997) recognized
the current river as a misfit within the sector of the original
catchment it still occupies.

The form and distribution of glacially transported and
deposited materials present throughout the area have been
established by the British Geological Survey's (BGS) mapping
programme in the region (e.g. BGS, 1989, 1993, 1994, 2003,
2006a,b, 2007a,b, 2008, 2010). These materials include
widespread diamicton of subglacial origin (till) and, princi-
pally along valley bottoms, extensive deposits of glaciofluvial
and glaciodeltaic sand and gravel, and glaciolacustrine silt
and clay. The presence of exotic igneous, metamorphic and
sedimentary rock clasts, as well as common shell fragments
and Cenozoic lignite particles, allow sediment derived from
the catchment region of Irish Sea ice to be distinguished from
Welsh ice-sourced materials that contain clasts only of the
regional Lower Palaeozoic bedrock (e.g. Davies *et al.*, 2003).
Several studies (e.g. Waters *et al.*, 1997; Hambrey *et al.*,
2001; Glasser *et al.*, 2004; Etienne *et al.*, 2006; Davies *et al.*,
2006b; Patton and Hambrey, 2009) have charted the advance
of the Irish Sea Ice Stream into western parts of the Teifi and
Aeron catchments and the evolution of pro- and sub-glacial
drainage features and spillways as the Ice Stream impounded
and then displaced glacial Llyn Teifi. Locally extensive sand
and gravel deposits, as worked for example at Trefigin,
Pantgwyn and Penparc quarries (Fig. 2B), are interpreted as
outwash formed during the subsequent recession of Irish Sea
ice from this region (see below). Conversely, the distribution
of Devensian deposits of Welsh Ice Cap provenance confirms
that much of the area away from the coastal tract lay within
the reach of the Welsh Ice Cap. The co-incidence of the
inland, eastern limit of abundant Irish Sea erratic material and
the western extent of Welsh ice-contact deposits indicate that
the two ice masses converged. However, Waters *et al.* (1997;
see also Jones, 1965 and Davies *et al.*, 2006b) suggested that,
at the time of the LGM, there remained an ice-free enclave
along the main Teifi valley; and the reconstructions of Etienne
et al. (2006) and Wilby *et al.* (2007) show this as the northern
point of an extensive and widening region to the south that
escaped Late Devensian glaciation (see below).

The southern Cambrian Mountains and the valleys of the
Teifi (including its major tributary, the River Dulas) and the
Aeron were the loci for regional ice discharge (Fig. 2; Jansson
and Glasser, 2005; Sahlin *et al.*, 2007; Sahlin, 2010). The
deposits and landforms formed during recession in these river
catchments were assessed during the BGS mapping of the
region (Davies *et al.*, 1997, 2006a,b; Waters *et al.*, 1997;
Ross, 2006; Wilby *et al.*, 2007; Burt *et al.*, 2012). Mounds
and hummocks of poorly stratified and poorly sorted ice-
contact sand and gravel record the location of cross-valley
and lateral moraines marking the retreat of discrete valley
glaciers that occupied these valleys during Devensian

deglaciation. Valley floor exposures and boreholes show that,
during glacier withdrawal, the recessional moraines in both
catchments impounded pro-glacial lakes in which clay,
silt and glaciodeltaic deposits accumulated (Merrin, 1999;
Davies *et al.*, 2006a,b). In the Teifi valley, the lake dammed
by the northernmost of these moraines evolved into Tregaron
Bog (Cors Caron in Welsh) — one of the largest raised peat
bogs in the UK (Godwin and Mitchell, 1938; Davies *et al.*,
1997). Radiocarbon dating at this site by Hibbert and Switsur
(1976) (10 200 ± 220 cal BP) confirms that organic-rich sedi-
ments began to accumulate above barren, grey, lacustrine
clays soon after the climatic amelioration that signalled
the end of the Younger Dryas Stadial and the onset of the
Holocene.

In upland and interfluve areas, glacially streamlined bed-
rock ridges show a strong structural bedrock control. Deposits
of head and nivation scree (head gravels) testify to the
periglacial conditions that prevailed as Devensian ice with-
drew from the region. Landslides, alluvial fans and river
terraces record paraglacial adjustment of the landscape that
preceded the establishment of the area's modern drainage
system and modern alluvial deposition (Davies *et al.*, 1997,
2006a).

Sampling strategy and sample details

Irish Sea Ice Stream deglaciation

Four sediment samples were obtained for luminescence
dating from two sand and gravel quarries located to the south
of the Teifi valley, SW of Cardigan: two samples from
Pantgwyn Quarry (MW05 and MW07; 52.048°N, 4.735°E)
and two samples from Trefigin Quarry (MW08 and MW09;
52.057°N, 4.718°E) (Fig. 3). Sample details are provided in
Tables 1 and 2. Both quarries work ridges of poorly sorted
gravel and coarse to fine sand, in which abundant cross-
stratification testifies to deposition by southerly flowing,
braided rivers (Fig. 3) (Owen, 1997). Clast assemblages and
abundant shell fragments confirm an Irish Sea Ice Stream
source. Extensional faulting (Fig. 3b) seen in the quarry faces
has been interpreted by Hambrey *et al.* (2001) as evidence of
collapse of the sediment pile following the decay of flanking
ice buttresses. Fining-upwards successions at both sites
further support their interpretation as remnants of a once
more extensive spread of glacial outwash formed during the
withdrawal of the Irish Sea Ice Stream from the area (e.g.
Davies *et al.*, 2003). Significantly, both quarries are located
several kilometres to the north of the Preseli Mountains,
which formed the local southern limit of the Irish Sea Ice
Stream advance into the region.

Welsh Ice Cap deglaciation

The absence of glacially transported boulders on the surface
of recessional moraines in the Teifi and Aeron valleys
precluded dating of these features using cosmogenic isotope
techniques. However, 10 samples were collected for cosmo-
genic nuclide exposure dating from glacially transported
boulders and ice-scoured bedrock sites located in the
adjacent uplands and interfluves (Table 3; Fig. 4). Following
the sampling guidelines of Gosse and Phillips (2001), Dunai
(2010) and Balco (2011), samples were collected from the
upper surfaces using a hammer and chisel and all samples
were <4 cm thick. Detailed site descriptions were made for
each sample. Skyline measurements were recorded using an
Abney level where the angle to the horizon was >15°.
Sample coordinates were collected using a handheld GPS
with a horizontal accuracy of ±4 m. The cosmogenic nuclide

Figure 3. Glaciofluvial sand and gravel, Trefigin Quarry: (a) sets of cross-bedded coarse to fine sand indicating current flow from the north; (b) planar- and cross-laminated sand disrupted by extensional faults. Hammer is 28 cm long. [Colour figure can be viewed at wileyonlinelibrary.com]

samples fall into two broad geographical groups: (i) those associated with the deglaciation of the Cambrian Mountain plateau and the eastern side of the Afon Teifi catchment (seven samples); and (ii) those associated with the deglaciation of the Afon Aeron catchment and the Mynydd Bach plateau (three samples). Sample locations are indicated on Fig. 2B, and further information relating to samples can be found in Tables 3 and 4.

Methods and results

Geomorphological mapping

Extensive geomorphological mapping was undertaken by BGS and its collaborators as part of their field investigations in the region (e.g. Waters et al., 1997; Hambrey et al., 2001; Glasser et al., 2004; Etienne et al., 2006; Davies et al., 2006b) and incorporated the results of earlier studies (e.g. Jones, 1965; Watson, 1969). Landforms and sediments were identified according to their size, shape, composition and texture using field observations, including section logging and hand augering, colour *stereo* aerial photography, borehole records and site investigation reports (see McMillan and Powell, 1999; Hubbard and Glasser, 2006).

Luminescence dating

Samples were taken for luminescence dating by hammering opaque tubes into the sedimentary section to prevent exposure to sunlight during sampling. External beta dose-rates were determined for optically stimulated luminescence (OSL) dating using inductively coupled plasma mass spectrometry (ICP-MS) and inductively coupled plasma atomic emission spectroscopy (ICP-AES), and the external gamma dose-rates were determined using *in situ* gamma spectrometry (Table 1). To isolate coarse-grained quartz for OSL analysis, each sample was first treated with a 10% (v/v) dilution of 37% HCl and with 20% (v/v) of H_2O_2 to remove carbonates and organics, respectively. Dry-sieving then isolated grains 180–212 μm in diameter, and density-separation using sodium polytungstate provided the 2.62–2.70 g cm^{-3} (quartz-dominated) fractions. The quartz grains were etched for 1 h in 40% hydrofluoric (HF) acid to remove the outer portion of the quartz grains that was affected by alpha irradiation and also remove any contaminating grains of feldspar. After the HF etching, grains were washed in a 10% solution of HCl to remove any fluorides that may have been produced. Grains were finally mounted into 10 × 10 grids of 300-μm-diameter holes in a 9.8-mm-diameter aluminium single-grain disc for analysis.

Table 1. Environmental dose-rates determined for OSL dating of single grains of quartz using ICP-MS analysis and field gamma spectrometry. The chemical concentrations are presented in the decimal points relevant for the detection limit. The dose-rates were calculated using the conversion factors of Guerin et al. (2011) and beta dose-rate attenuation factors of Guérin et al. (2012). Water-contents (17 ± 5%) were estimated considering the field and saturated water contents, and the environmental history for each sample; these values are expressed as a percentage of the mass of dry sediment. Cosmic dose-rates were determined after Prescott and Hutton (1994), using a depth of 3 ± 2 m for all samples. Dose-rates were calculated using the dose rate and age calculator (DRAC; Durcan et al., 2015). All samples have a laboratory prefix code (Aber210/).

Sample	K (%)	Rb (ppm)	U (ppm)	Th (ppm)	Beta dose-rate (Gy ka^{-1})	Gamma dose-rate (Gy ka^{-1})	Cosmic dose-rate (Gy ka^{-1})	Total dose-rate Gy ka^{-1}
MW05	0.8 ± 0.1	35.7 ± 3.6	1.15 ± 0.12	3.6 ± 0.4	0.66 ± 0.06	0.37 ± 0.03	0.14 ± 0.01	1.19 ± 0.07
MW07	1.1 ± 0.1	46.2 ± 4.6	1.09 ± 0.11	4.1 ± 0.4	0.85 ± 0.08	0.45 ± 0.03	0.14 ± 0.01	1.46 ± 0.09
MW08	1.1 ± 0.1	47.5 ± 4.8	1.21 ± 0.12	4.4 ± 0.4	0.87 ± 0.08	0.61 ± 0.04	0.14 ± 0.01	1.63 ± 0.09
MW09	0.8 ± 0.1	34.3 ± 3.4	0.88 ± 0.09	3.2 ± 0.3	0.63 ± 0.06	0.40 ± 0.03	0.14 ± 0.01	1.18 ± 0.07

Table 2. OSL analysis results, including the dose-recovery (DR) overdispersion (OD).

Sample	Site	Total analysed	n	OD (%)	Age model	D_e (Gy)	Age (ka)	Weighted mean age (ka)
MW05	Pantgwyn	3000	61	58 ± 1	MAM	34.6 ± 4.6	29.1 ± 4.2	26.7 ± 1.8
MW07	Pantgwyn	1900	59	30 ± 1	CAM	38.3 ± 1.8	26.2 ± 2.0	
MW08	Trefigin	2400	108	29 ± 1	CAM	46.0 ± 1.6	28.1 ± 1.9	26.7 ± 1.6
MW09	Trefigin	2900	54	59 ± 1	MAM	26.9 ± 3.4	22.8 ± 3.2	

All luminescence measurements were performed using a Risø TL/OSL DA-15 automated single-grain system equipped with a ^{90}Sr/^{90}Y beta source (Bøtter-Jensen *et al.*, 2003) as described by Smedley *et al.* (2017a,b) . A preheat plateau test performed on 5-mm aliquots was used to determine the preheat temperature used (200 °C) with a cutheat of 160 °C for the single aliquot regenerative dose (SAR) protocol (Murray and Wintle, 2000). Five screening criteria were applied to the resulting data throughout the analyses unless otherwise specified. Grains were screened based upon whether (i) the test dose response was greater than three sigma above the background, (ii) the test dose uncertainty was <20%, (iii) the recycling and OSL-IR depletion ratios were within the range of ratios 0.8–1.2, (iv) recuperation was <5% of the response from the largest regenerative dose (150 Gy) and (v) the single-grain equivalent dose (D_e) values were not from a population of very low doses that were identified by the finite mixture model (FMM) to be inconsistent with the geological context of the sample (i.e. <1 ka). The associated uncertainties were taken into account when applying the screening criteria. D_e values were then calculated for all grains that passed the screening criteria, incorporating the uncertainty from instrument reproducibility of 2.5% (Thomsen *et al.*, 2005). Dose-recovery experiments were performed on Samples MW05 (overdispersion = 16 ± 1%), MW07 (overdispersion = 22 ± 1%) and MW09 (overdispersion = 15 ± 1%) and suggested that the SAR protocol was appropriate for OSL dating. The single-grain D_e values determined for each sample are shown (Fig. 5) and included in Appendix 1.

Luminescence dating results

The single-grain D_e distributions for Samples MW07 and MW08 were not asymmetrical and so the sediments were deemed to have been well bleached before burial; thus, the central age model (CAM) was used to determine D_e values for these samples (Table 2). The single-grain D_e distributions of Samples MW05 and MW09 were asymmetrically distributed and so the sediments were deemed to have been heterogeneously bleached before burial; thus, the minimum

age model (MAM) was used to determine D_e values for these samples (Table 2). The overdispersion arising from intrinsic OSL characteristics for each sample was combined in quadrature with the overdispersion arising from external microdosimetry (20%) to determine the values of σ_b used for the MAM ($\sigma_b = 0.25$). The D_e values were then divided by the environmental dose-rates to determine OSL ages (Table 2). The weighted mean and standard error (eqns 21 and 22 in Aitken and Alldred, 1972) of the two OSL ages at both Pantgwyn and Trefigin were 26.7 ± 1.8 and 26.7 ± 1.6 ka, respectively; consistent with their proximity to one another, these ages appear to confirm that outwash accumulation at both sites was broadly synchronous.

Cosmogenic nuclide dating

Samples were processed in the Natural Environment Research Council (NERC) Cosmogenic Isotope Laboratory Facility, at the Scottish Universities Environmental Research Centre (SUERC). After the mechanical procedures and chemical etching to separate the quartz from other minerals and remove the meteoric ^{10}Be, the pure quartz was spiked with ^{9}Be (approx. 0.2 mg ^{9}Be) and ^{27}Al (to total up ~1500 mg ^{27}Al) and dissolved. The beryllium and aluminium isotopes were extracted following chemical procedures adapted from Child *et al.* (2000). Prepared BeO and AlO targets were subsequently mixed with Nb and Ag, respectively, and pressed into copper cathodes. Target measurements were performed using the 5-MV accelerator mass spectrometer at the SUERC AMS Laboratory (Xu *et al.*, 2010). Measured ^{10}Be/^{9}Be ratios and ^{26}Al/^{27}Al ratios were converted to nuclide concentrations in quartz and exposure ages were calculated using the Cronus Earth online calculator v.2.3 (hess.ess.washington.edu/; Balco *et al.*, 2008). The calculated age uncertainties are expressed as ±1σ (Table 4). Internal uncertainties are quoted when describing our results and the external uncertainties are quoted when comparing our results to previously published data sets.

A range of ^{10}Be production rates can be used to calculate exposure ages and there remain uncertainties over suitable

Table 3. Location and details of samples collected for cosmogenic isotope dating (see also Fig. 4).

| Sample	Latitude (°N)	Longitude (°W)	Altitude (m)	Thickness (cm)	Density (g cm^{-3})	Shielding (factor)
AV1201	52.288332	4.04284773	339	2	2.65	1
AV1202	52.249909	4.04783623	347	2	2.65	1
BB1201	52.180370	3.889437	370	2	2.65	1
BB1202	52.189138	3.902756	466	2	2.65	1
CT1201	52.114032	3.977533	371	2	2.65	1
MP1201	52.063093	4.087965	392	2	2.65	1
TP1203	52.293819	3.76683368	435	2	2.65	1
TV1201	52.288467	3.91515499	290	2	2.65	1
YST1201	52.340828	3.7616162	497	3	2.65	1
YST1202	52.340809	3.7616595	495	4	2.65	1
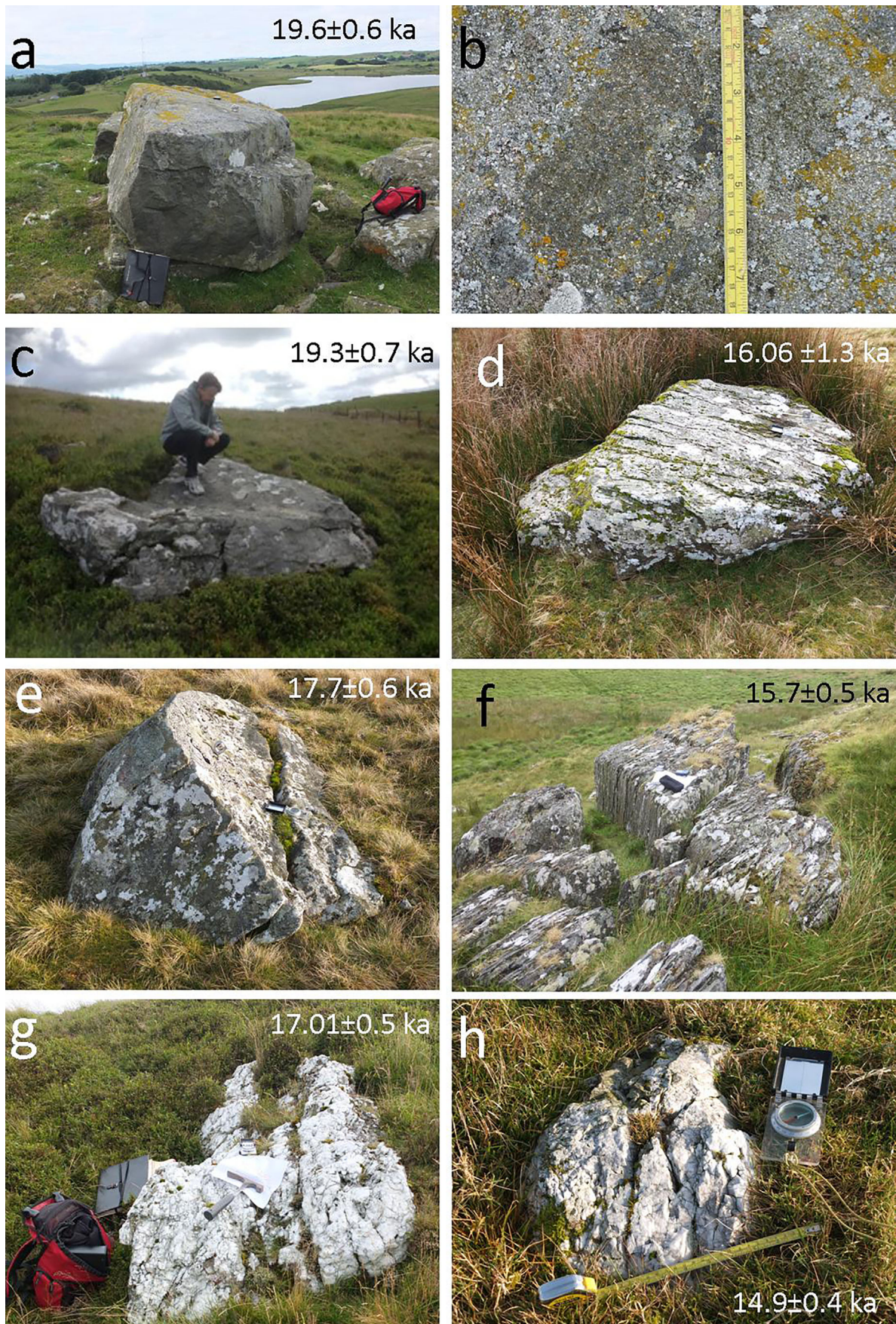
Figure 4. Photographs of selected sites sampled for cosmogenic dating (see Fig. 2 and Table 3 for location details): (a) Sample AV12/01, Hafod Ithel, Mynydd Bach (map case is 30 cm); (b) close up of quartz and feldspar granules at sampled point on a; (c) Sample CT 12/01, Craig Twrch, Cambrian Mountains; (d) Sample BB12/01, Blaenbrefi, Cambrian Mountains (max. length of boulder 1.8 m); (e) Sample BB12/02, Bryn Rhud, Cambrian Mountains (open compass is 18 cm long) (f) Sample TP12/03, Teifi Pools, Cambrian Mountains (GPS is 16 cm long); (g) Sample YST12/02, Banc Hir, Cambrian Mountains (hammer is 28 cm long); (h) TV12/01, Drysgol, region of Aeron-Teifi interfluve. Internal uncertainty values are shown for each sample. [Colour figure can be viewed at wileyonlinelibrary.com]

Table 4.   Concentrations and exposure ages of the samples collected for cosmogenic isotope dating.

Sample	AMS ID (Be)	AMS ID (Al)	^{10}Be concentrations 10Be $\pm \sigma$ (atoms g^{-1} quartz)	^{26}Al concentrations ^{26}Al $\pm \sigma$ (atoms g^{-1} quartz)	^{10}Be ages Exposure age (years)	Internal σ (years)	External σ (years)	^{26}Al ages Exposure age (years)	Internal σ (years)	External σ (years)
AV1201	b7903	a2224	117 152 ± 3377	815 134 ± 38 071	19 601	568	888	20 154	951	1184
AV1202	b7906	a2225	114 897 ± 3850	774 727 ± 49 149	19 082	642	924	19 007	1217	1387
BB1201	b7907	a2226	98 822 ± 7804	664 914 ± 201 483	16 063	1274	1391	15 955	4873	4905
BB1202	b7908	a2227	118 894 ± 3968	817 728 ± 69 440	17 718	594	856	18 008	1543	1666
CT1201	b7909	a2228	118 715 ± 4341	836 524 ± 72 645	19 299	709	977	20 100	1763	1898
MP1201	b7910	a2230	86 517 ± 4785	811 657 ± 132 780	13 780	765	903	19 127	3159	3229
TP1203	b7912	a2231	102 808 ± 3298	755 067 ± 54 878	15 741	507	746	17 083	1252	1387
TV1201	b7913	a2232	85 159 ± 2355	590 286 ± 27 900	14 898	414	663	15 238	726	900
YST1201	b7914	a2233	97 649 ± 3013	775 413 ± 38 409	14 246	441	663	16 722	835	1019
YST1202	b7915	a2234	115 985 ± 3124	875 356 ± 43 940	17 099	463	754	19 084	967	1175

The ratios ranged between 3.20×10^{-14} and 1.88×10^{-13} for ^{10}Be/^{9}Be, and between 1.26×10^{-13} and 4.18×10^{-13} for ^{26}Al/^{27}Al.
The ^{10}Be concentrations are corrected for the procedural blank values of 5.1615×10^{-13} and 5.8032×10^{-15}. Data relative to NIST SRM 4325 (^{10}Be/^{9}Be taken as 2.79×10^{-11}; Nishiizumi et al., 2007).
The ^{26}Al concentrations are corrected for the procedural blank values of 2.65×10^{-15} and 3.56×10^{-13}. Data relative to Z92-0222 (^{26}Al/^{27}Al taken as 4.11×10^{-11}; Nishiizumi, 2004).
Exposure ages calculated using Cronus-Earth ^{10}Be–^{26}Al exposure age calculator v.2.3 (hess.ess.washington.edu/). They assume zero erosion, scaling factors according to Stone (2000) and a spallation production rate of 4.49 ± 0.15 atom (g SiO$_2$)$^{-1}$ a^{-1} (Balco et al., 2008).
Uncertainties ($\pm 1\sigma$) include all known sources of analytical error.

values for Wales. To compare with other published data, we used the same ^{10}Be production rate for west Wales and the Irish Sea area as Chiverrell et al. (2013) to calculate ages: 4.20 ± 0.15 atoms g^{-1} a^{-1}. This production rate value is based on a calibrated dataset from north-west Scotland (Ballantyne and Stone, 2012). The ^{10}Be ages were calculated using the Lal (1991)/Stone (2000) production rate model. Exposure ages (Table 4) were calculated using a ^{10}Be decay constant of 4.99×10^{-7} a^{-1}, based on the half-life value of 1.387 ± 0.012 Myr (Chmeleff et al., 2010; Korschinek et al., 2010), and Stone scaling (Stone, 2000) to sampling site for both spallation and muon production. Previously published ^{10}Be ages from the neighbouring Aran mountains (Glasser et al., 2012) were recalculated using the same approach with the same range of production rates to enable direct comparison.

Cosmogenic nuclide dating results

Both the ^{10}Be and the ^{26}Al concentrations were calculated to explore the possibility of multiple exposure histories on the sampled rocks. For most of the samples in this study, the ^{26}Al/^{10}Be ratios are not depleted with respect to the production rate ratio of 6.75, suggesting a simple continuous exposure with no periods of burial since ice recession (Table 4). However, for two samples (MP12/01 and YST12/01), wide discrepancies in the ^{10}Be and ^{26}Al ages may indicate more complex histories of exposure (see below). Apparent ^{10}Be and ^{26}Al ages range between 14.3 ± 0.4 and 19.6 ± 0.6 ka. As the individual sample ^{10}Be and ^{26}Al ages are not statistically the same for all, we have not included the ^{26}Al ages in the discussion.

Discussion

Irish Sea Ice Stream deglaciation

The OSL ages obtained for the Pantgwyn and Trefigin deposits constrain the onset of this deglaciation. Significantly, they indicate that Irish Sea ice had withdrawn from the

foothills of the Preseli Mountains as far north as these sites by $\sim 26.7 \pm 1.6$ ka. These findings are consistent with the timing of ice impingement on the Isles of Scilly at 26–25 ka, suggesting that retreat from the maximum in the Celtic Sea occurred rapidly (i.e. within the uncertainties of the ages determined).

Welsh Ice Cap deglaciation in the Teifi Valley and Cambrian Mountains

Most of this sample set came from the eastern side of the Afon Teifi catchment, along the western flanks of the Cambrian Mountains plateau (Figs 2 and 6). These dates provide evidence for the age and pattern of the Welsh Ice Cap withdrawal across this upland region. The ages and locations of Samples CT12/01 (19.3 ± 0.7 ka), BB12/01 (16.1 ± 1.3 ka), BB12/02 (17.7 ± 0.6 ka), TP12/03 (15.7 ± 0.5 ka) and YST12/02 (17.1 ± 0.5 ka) tell a broadly consistent story. They suggest that ice withdrew from some of the most prominent upland ridges at c. 19 ka in the south of the region, exemplified by Criag Tyrch. This was preceded by a more widespread westwards retreat of the ice cap from the southern Cambrian Mountains towards the Teifi Valley, which was largely complete by c. 16–17 ka (Fig. 6).

Sample MP12/01 (13.8 ± 0.8 ka) is the most southerly sample of the Teifi Valley/Cambrian Mountains set. This sample, collected at a higher elevation (392 m) than others to the north, implies that the withdrawal of ice from this site was delayed until around 13.8 ka (Fig. 6). Whereas the other samples of this set provide a fairly consistent picture for the timing and pattern of ice retreat from the western flanks of the Cambrian Mountain plateau (see below), the date obtained for Sample MP12/01 appears to be an outlier. The mean exposure age provided by the northernmost sample, YST12/01 (14.3 ± 0.4 ka), in being significantly younger (~ 2.9 kyr) than that obtained for the nearby Sample YST12/02, also appears aberrant. For MP12/01 and YST12/01, the wide discrepancies between the Be and Al exposure data imply that both these samples may record a more complex exposure

history than other locations. The sample sites for MP12/01 and YST12/01 both exhibit features consistent with periglacial heaving and post-glacial downslope movement, which may explain this discrepancy.

Welsh Ice Cap deglaciation in the Aeron Valley and Mynydd Bach

The ages obtained for Samples AV12/01 (19.6 ± 0.6 ka) and AV12/02 (19.1 ± 0.6 ka) testify to the early emergence of the highest part of the Mynydd Bach plateau and indicate withdrawal of the Welsh Ice Cap from the whole of this upland region was complete by c. 19–20 ka. Sample TV12/01 (14.9 ± 0.4 ka) implies that, in common with much of the

Cambrian Mountains, the interfluve between the Teifi and Aeron catchments was similarly ice-free by c. 15 ka.

Integrating the geomorphological and geochronological evidence

In Figs 6 and 7 we present a putative chronology and palaeogeographical model for the deglaciation of south-west Wales in the context of late Pleistocene climate events including those identified by the Greenland-based 'INTIMATE' project (e.g. Björck et al., 1998; Blockley et al., 2014). The regional maximum limits of the Irish Sea Ice Stream and Welsh Ice Cap in the region are based, with only minor modification, on published accounts (e.g.
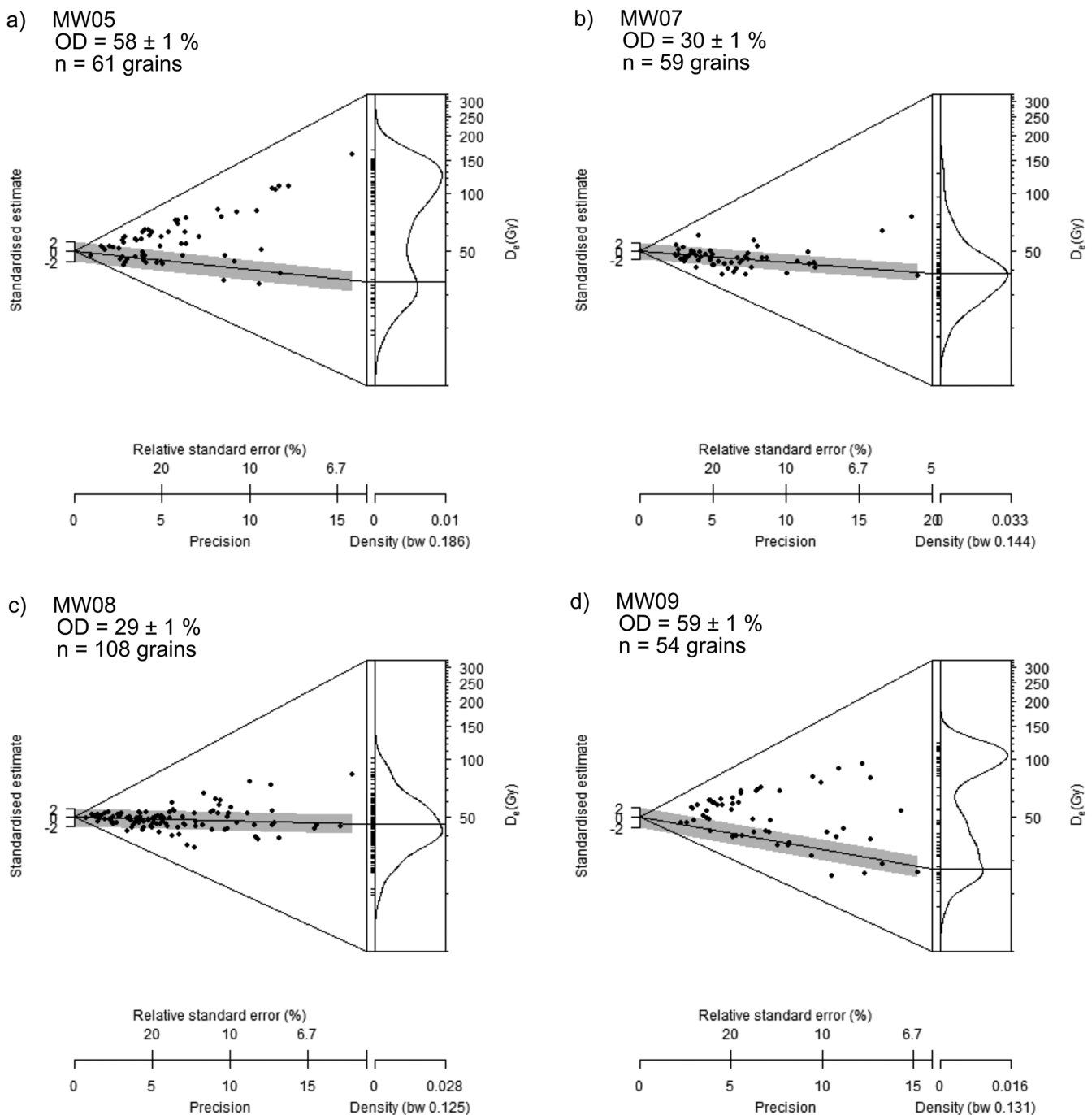

Figure 5. Abanico plots showing the single-grain D_e values determined for OSL dating, where the grey shading marks the CAM or MAM D_e value ($\pm 2\sigma$).

Waters *et al.*, 1997; Davies *et al.*, 2006b; Etienne *et al.*, 2006; Wilby *et al.*, 2007). The absence of obvious end moraines along the Teifi Valley probably reflects the termination of both ice masses in the surviving remnant of Llyn Teifi. Waters *et al.* (1997) follow Jones (1965) in suggesting that benches of sand and gravel near Pentre-Cwrt are the remnants of a former delta − the Pentre Cwrt Delta − that built out into the lake close to the Welsh Ice Cap's terminal position (Fig. 6).

The succession of ice-retreat lines shown on Fig. 6 are constrained by the new exposure ages and geomorphological evidence. The latter, including cross-valley moraines (numbered on Fig. 6), kame terraces, glaciolacustrine basins, and remnant deltas and outwash plains, chart the early withdrawal of both ice masses from the coastal tract and show that the subsequent deglaciation of the area was interrupted by episodes of stagnation or re-advance. The new OSL dates for Irish Sea glacial outwash are consistent with the early retreat of this western, maritime component of the BIIS in response to post-glacial maximum climatic amelioration perhaps linked to the INTIMATE GI-3 event. Its withdrawal from the Preseli Mountains and lower Teifi valley areas was evidently well advanced by *c.* 26 ka. Glacial deposits and landforms preserved to the north provide a record of the decoupling of the Irish Sea Ice Stream from the Welsh Ice Cap and the local impounding of temporary lakes between the separating ice masses (Davies *et al.*, 2006b; Ross, 2006). The eroded remnants of associated glaciofluvial fan deltas supplied by meltwater from the Irish Sea Ice Stream to the north, as for example at Talgarreg, locally allow the position of the retreating ice front to be reconstructed with some precision.

The later deglaciation of Welsh ice from Mynydd Bach and parts of the southern Cambrian Mountains saw the early emergence of bedrock prominences such as Hafod Ithel (Sample AV12/01) and Craig Twrch (Sample CT12/01). This marked the onset of a period of rapid reconfiguration of distal parts of the Welsh Ice Cap at *c.* 20–19 ka, which resulted in the formation of discrete Teifi and Aeron valley outlet glaciers. By this time, the Irish Sea Ice Stream had fully decoupled from the Welsh Ice Cap and was positioned on the northern Llŷn Peninsula (Smedley *et al.*, 2017b) and both ice masses had completely vacated the coastal tract of south-west Wales. Significant Welsh ice withdrawal from the lower Teifi Valley had probably already occurred (Figs 6 and 7) and the early retreat moraine T1 had formed and been abandoned. Deglaciation during this interval occurred during the climatic flux associated with the GS-3 to GS-2.1 INTIMATE events.

The extensive kamiform deposits and associated cross-valley moraines (T2-3) to the east of Llandysul mark the onset of this process in the Teifi Valley. Comparable landforms suggest that withdrawal of the Welsh Ice Cap outlet glaciers that occupied the lower reaches of the Aeron (A1), Ystwyth (Y1) and Rheidol (R1) valleys was also in progress from around this time (Fig. 6). Glacier recession from the Aeron Valley was subsequently interrupted by episodes of stagnation or re-advance on at least two occasions (A2–3), but the succession of landforms seen along the Teifi and Dulas valleys provides evidence of a longer period of ice occupation and of a staggered glacial retreat that halted on at least a further nine occasions (T4–12, D1–4). Although a precise chronology for these events remains difficult to tie down, the new cosmogenic exposure ages provide a basis for a provisional interpretation and comparison with the Greenland-based INTIMATE climate events (Figs 6 and 7). A majority of the Cambrian Mountain dates describe a

westwards withdrawal of ice from the upland plateau towards the axis of the Teifi Valley. Sample TV12/01 indicates that by 14.9 ka ice had also withdrawn from the region of the Aeron–Teifi interfluve and it is likely that the whole of the western sector of the study area including the Aeron Valley may then have been ice-free (Fig. 6).

Glacial landforms between Llandysul and Tregaron Bog reveal a staged northwards recession of the Teifi glacier along this 45-km-long reach of the valley (Figs 6 and 7). Recession of the ice from the Teifi valley probably commenced soon after the decoupling of Irish Sea ice from the Welsh Ice Cap, ongoing before 19 ka (see above). The chronology of its subsequent retreat is constrained ostensibly by the MP12/01 exposure age (13.8 ± 0.8 ka) in the south and, in the north, by the onset of early post-glacial deposition at Tregaron Bog (10.2 ka). However, Late Devensian ice is widely assumed to have disappeared from Wales, as throughout much of the UK, during the early part of the Windermere Interstadial *c.* 13.5 cal ka (Clark *et al.*, 2012). Even the maximum interval these figures allow (*c.* 1700 years) appears too short to generate the complex suite of recessional landforms and deposits preserved to the south of Tregaron Bog. Such analysis underlines the probability that the cosmogenic isotope values obtained for Sample MP12/01 may not accurately reflect the date of ice withdrawal from this locality (see above).

The exposure age obtained for Sample TV12/01 (*c.* 14.9 ka) offers an alternative, more realistic chronology arguably more consistent with other data. Its proximity to Tregaron Bog implies that the withdrawal of ice from this sample site can be linked to the recession of the Teifi glacier into the area currently occupied by the bog and to the formation of its associated recessional moraines (T11 and T12; Fig. 6). Hence, and contrary to MP12/01, it suggests that much of the 45-km northwards retreat of the Teifi Valley Glacier into the Tregaron area spanned a period of over 5000 years (Fig. 7). The succession of cross-valley moraines and impounded lake deposits formed during this interval undoubtedly testify in some way to the impact of climatic variations associated with the INTIMATE GS-2.1a-b interval. However, the dynamic nature of the glacier probably meant that its response to these events was neither synchronous nor simplistic.

The absence of recessional moraines to the north of Tregaron Bog appears to signal a marked change in ice behaviour and that the final phase of ice withdrawal from the upper reaches of the modern and palaeo-Teifi valleys was rapid and uninterrupted. This must have occurred between *c.* 14.9 ka and *c.* 13.5 ka in response to the climatic amelioration associated with the Windermere Interstadial (= INTIMATE GI-1) (Fig. 7). The undated lacustrine clays present beneath the organic-rich Holocene sediments at Tregaron Bog may include material laid down during this period of warming or the subsequent, short-lived, cold period (Loch Lomond Stadial/Younger Dryas; INTIMATE event GS-1), as at other sites in mid-Wales (e.g. Walker *et al.*, 2001).

The 10 cosmogenic nuclide exposure age samples from these valleys provide the first chronological control on landforms related to the terrestrial deglaciation of south-west Wales. They indicate that deglaciation was well underway by 19 ka and that discrete outlet glaciers subsequently occupied and receded up the Aeron and Teifi valleys. By 15 ka these glaciers had retreated into the uplands of Wales and the lower reaches of these valleys were ice-free. Glasser *et al.* (2012) and Hughes *et al.* (2016) presented [10]Be exposure ages from mountain summits in the Aran Mountains, the northern Rhinogydd, the Moelwyns and the Arenigs of North Wales and used these to establish the vertical exposure history of the Welsh Ice Cap. Their exposure ages indicate a
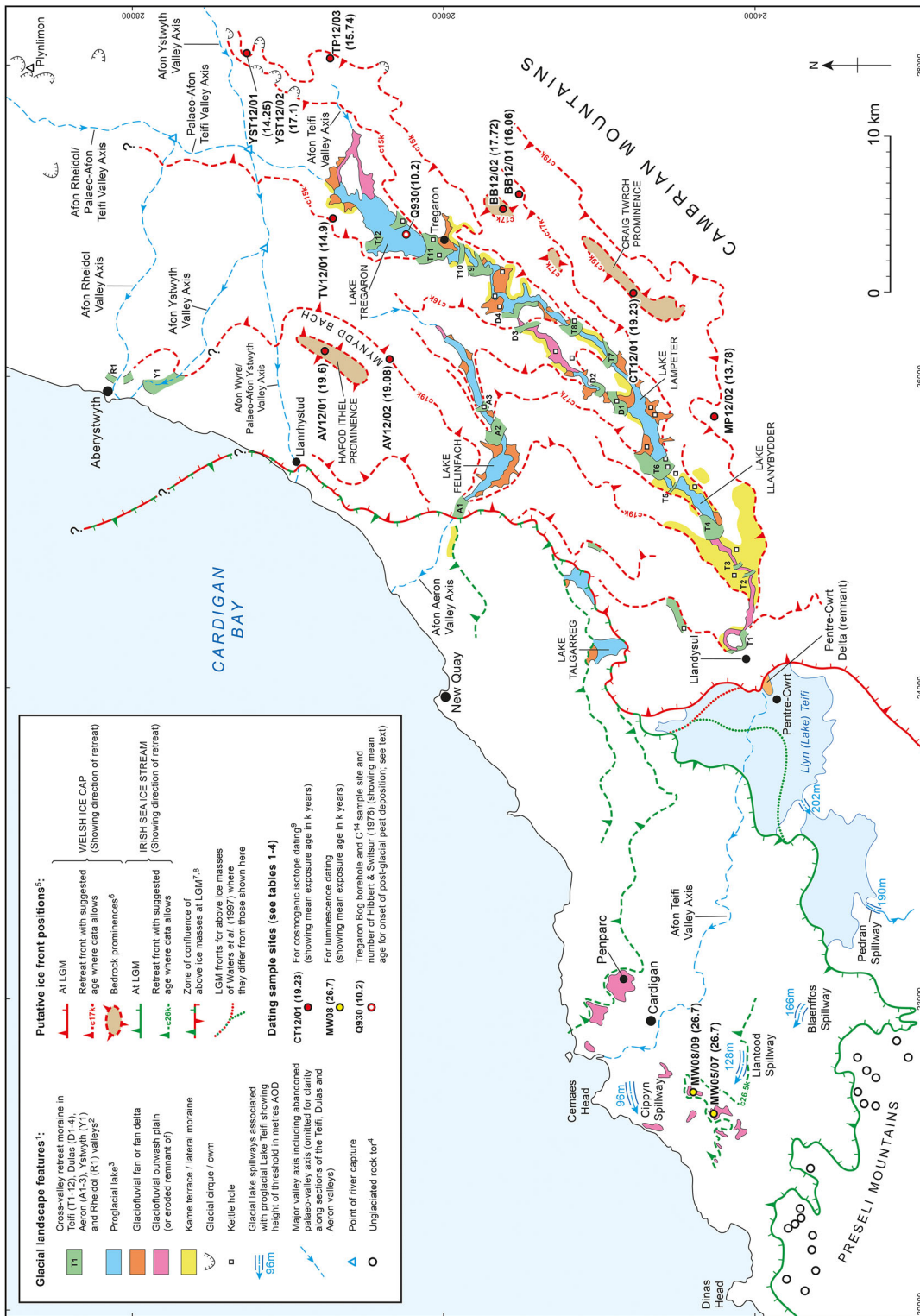
Figure 6. Integrated geomorphological and deglaciation model for the Welsh Ice Cap and Irish Sea Ice Stream in south-west Wales showing putative ice fronts at the Last Glacial Maximum (LGM) and at stages during their retreat, based on published maps of glacial deposits (see text) and the new OSL and cosmogenic isotope ages presented in this paper. Notes: 1. Some geomorphological features have been extrapolated to show their likely extent before later Pleistocene and Holocene deposition and erosion. 2. Only the most seaward of the retreat moraines present in the Ystwyth and Rheidol valleys are shown. 3. Only the largest proglacial lakes are named – many of the others were probably short-lived features that drained rapidly as their moraine dams were breached soon after ice withdrawal. 4. 'Unglaciated' refers only to the Late Devensian – the Preseli Mountains were over-ridden during earlier, more extensive episodes of Pleistocene ice advance. 5. Ice-front positions incorporate and update those proposed in the area by Davies et al. (1997, 2006b), Waters et al. (1997), Etienne et al (2006), Wilby et al. (2007) and Burt et al. (2012). 6. Bedrock prominences indicate those areas that were the first to emerge from under the Welsh Ice Cap (WIC) during thinning. 7. As independently evolving ice masses, the maritime Irish Sea Ice Stream and the land-based WIC need not have achieved their maximum extents in the region at the same time (e.g. Patton et al., 2013c). The WIC may have continued to advance westwards along the Afon Teifi valley, and to the south, for some time after the Irish Sea Ice Stream had attained its maximum limit in the region. 8. The new ages and their interpretation imply that the maximum advance of the Irish Sea Ice Stream into south-west Wales occurred before 26.7 ka and that this ice mass had fully decoupled from the WIC and withdrawn from the region before c. 20 ka. 9. Dates obtained for Samples MP12/01 and YST12/01 are not considered to represent maximum exposure ages – see text for full explanation. [Colour figure can be viewed at wileyonlinelibrary.com]
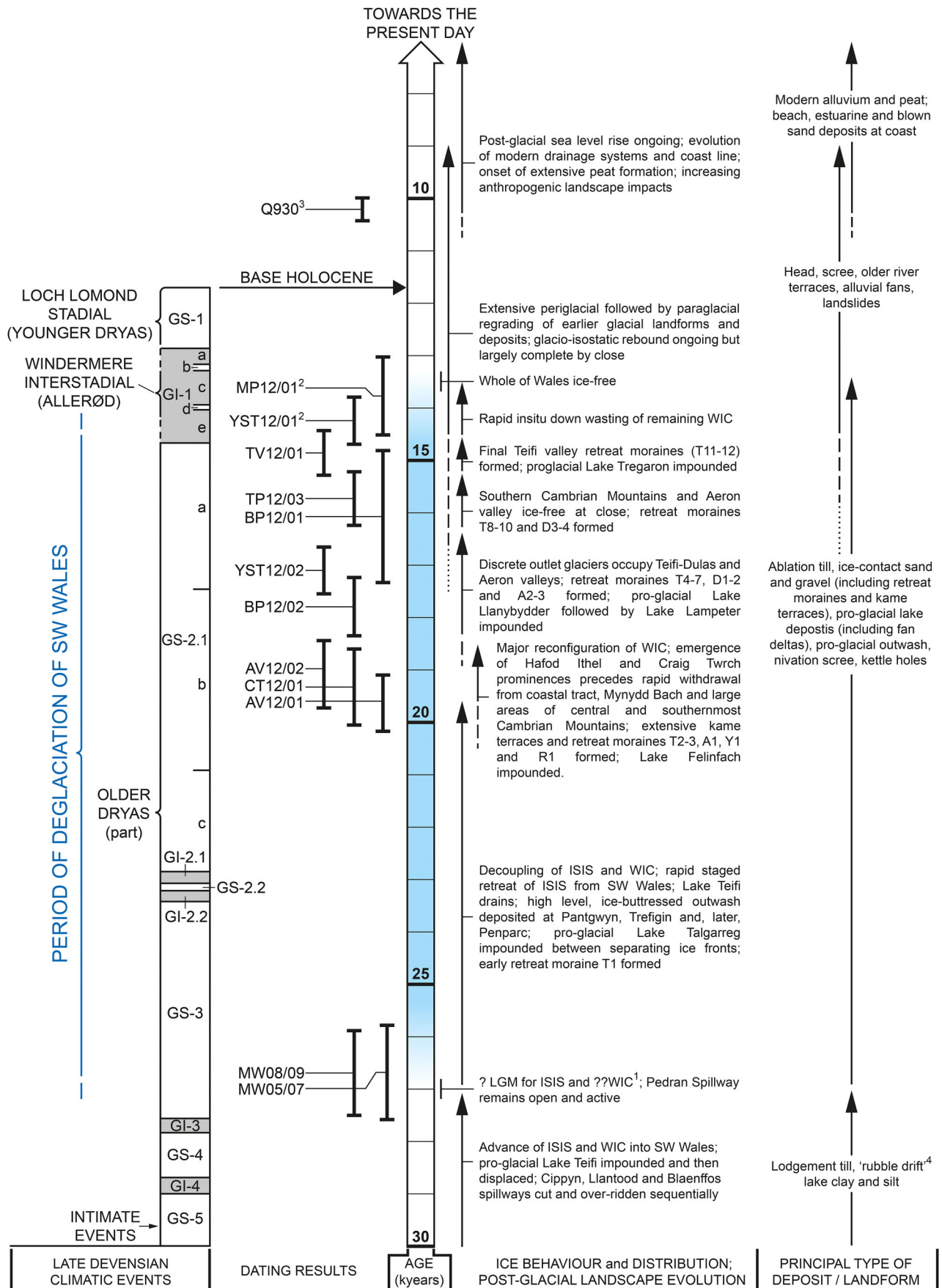
TOWARDS THE
PRESENT DAY

LATE DEVENSIAN CLIMATIC EVENTS

LOCH LOMOND STADIAL (YOUNGER DRYAS) — GS-1

WINDERMERE INTERSTADIAL (ALLERØD) — GI-1 (a, b, c, d, e)

PERIOD OF DEGLACIATION OF SW WALES

GS-2.1 (a, b, c)

OLDER DRYAS (part)

GI-2.1
GS-2.2
GI-2.2

GS-3

GI-3
GS-4
GI-4

INTIMATE EVENTS — GS-5

DATING RESULTS

Q930[3]
MP12/01[2]
YST12/01[2]
TV12/01
TP12/03
BP12/01
YST12/02
BP12/02
AV12/02
CT12/01
AV12/01
MW08/09
MW05/07

AGE (kyears)

BASE HOLOCENE

10
15
20
25
30

ICE BEHAVIOUR and DISTRIBUTION; POST-GLACIAL LANDSCAPE EVOLUTION

Post-glacial sea level rise ongoing; evolution of modern drainage systems and coast line; onset of extensive peat formation; increasing anthropogenic landscape impacts

Extensive periglacial followed by paraglacial regrading of earlier glacial landforms and deposits; glacio-isostatic rebound ongoing but largely complete by close

Whole of Wales ice-free

Rapid insitu down wasting of remaining WIC

Final Teifi valley retreat moraines (T11-12) formed; proglacial Lake Tregaron impounded

Southern Cambrian Mountains and Aeron valley ice-free at close; retreat moraines T8-10 and D3-4 formed

Discrete outlet glaciers occupy Teifi-Dulas and Aeron valleys; retreat moraines T4-7, D1-2 and A2-3 formed; pro-glacial Lake Llanybydder followed by Lake Lampeter impounded

Major reconfiguration of WIC; emergence of Hafod Ithel and Craig Twrch prominences precedes rapid withdrawal from coastal tract, Mynydd Bach and large areas of central and southernmost Cambrian Mountains; extensive kame terraces and retreat moraines T2-3, A1, Y1 and R1 formed; Lake Felinfach impounded.

Decoupling of ISIS and WIC; rapid staged retreat of ISIS from SW Wales; Lake Teifi drains; high level, ice-buttressed outwash deposited at Pantgwyn, Trefigin and, later, Penparc; pro-glacial Lake Talgarreg impounded between separating ice fronts; early retreat moraine T1 formed

? LGM for ISIS and ??WIC[1]; Pedran Spillway remains open and active

Advance of ISIS and WIC into SW Wales; pro-glacial Lake Teifi impounded and then displaced; Cippyn, Llantood and Blaenffos spillways cut and over-ridden sequentially

PRINCIPAL TYPE OF DEPOSIT / LANDFORM

Modern alluvium and peat; beach, estuarine and blown sand deposits at coast

Head, scree, older river terraces, alluvial fans, landslides

Ablation till, ice-contact sand and gravel (including retreat moraines and kame terraces), pro-glacial lake depostis (including fan deltas), pro-glacial outwash, nivation scree, kettle holes

Lodgement till, 'rubble drift'[4] lake clay and silt

Figure 7. Timeline for the deglaciation of south-west Wales as suggested by the dating results of this study (see Tables 1–4 and Fig. 6) in the context of late Pleistocene climatic intervals including the Greenland Ice Sheet INTIMATE events (see text). Notes: 1. See Fig. 6, note 6. 2. Dates obtained for these samples are not considered to represent maximum exposure ages – see text. 3. Sample of Hibbert and Switsur (1976) that dates the onset of post-glacial, organic-rich sediment accumulation at Tregaron Bog. 4. See Hambrey *et al.* (2001). Dotted, dashed and solid vertical arrows are used to imply increasing significance of process or landform. Abbreviations: ISIS = Irish Sea Ice Stream; WIC = Welsh Ice Cap. [Colour figure can be viewed at wileyonlinelibrary.com]

clear pattern demonstrating that, following a period of rapid thinning, mountain summits in North Wales became exposed as nunataks between 19 and 20 ka. Our samples from the Cambrian Mountain are farther south and at lower elevations than those collected in North Wales. Nevertheless, our [10]Be exposure ages appear to confirm that there was a period of significant thinning around 20 ka, that bedrock prominences became emergent around this time, and that deglaciation of the south-west portion of the Welsh Ice Cap was then dominated by a series of increasingly discrete outlet glaciers that receded progressively up-valley. Numerical ice-sheet models show a similar recessional pattern, with dynamic outlet glaciers occupying valleys during deglaciation as the ice cap receded into the interior of Wales (Patton *et al.*, 2013a,b,c).

These new data from the south-west of the Welsh Ice Cap are also relevant to the debate about the extent of the ice cap at the LGM. In a series of papers, Watson (1965, 1969) argued that this area of mid-Wales is predominantly a periglacial landscape, lacking evidence of glaciation. Watson argued that, where they exist, glacial deposits are buried beneath periglacial landforms and sediments implying that there was a period of prolonged or intense periglacial activity following glaciation. However, our geomorphological mapping and associated [10]Be exposure ages indicate that upland areas in south-west Wales share a similar deglaciation history to mountainous regions in North Wales, that valley glaciers remained active in the region until *c.* 15 ka, and that their subsequent recession into upland source areas and final down-wasting pre-dated the Windermere Interstadial. Evidence for a regionally widespread or significantly more protracted Late Devensian periglacial phase is therefore lacking.

Conclusions

i. Using luminescence and cosmogenic isotope dating, we have produced the first detailed chronological framework for Late Devensian glacial events in south-west Wales and the southern Cambrian Mountains.

ii. Luminescence ages for ice-contact sand and gravel deposits at Pantgwyn and Trefigin of 26.7 ± 1.8 and 26.7 ± 1.6 ka, respectively, indicate that the Irish Sea Ice Stream was undergoing active recession from the coastal fringes of south-west Wales at that time and, consequently, that the maximum advance of the Irish Sea Ice Stream into south-west Wales occurred before this.

iii. Deglaciation of the south-western area of the Welsh Ice Cap was marked by a progression from ice cap conditions to valley glaciation as the ice cap thinned and its outlet glaciers became increasingly constrained by the local topography.

iv. Deglaciation of the Welsh Ice Cap probably commenced immediately after the LGM. Bedrock prominences were the first features to emerge from the ice cover. By 19 ka, the adjacent upland regions were ice-free and outlet glaciers occupied, and had begun to recede up, the Aeron and Teifi valleys. By this time, the Irish Sea Ice Stream had fully decoupled from the Welsh Ice Cap and both ice masses had probably withdrawn from the coastal tract of south-west Wales.

v. Cross-valley recessional moraines and glacial lake and outwash sediments chart multiple periods of stagnation or re-advance of the Teifi and Aeron glaciers. By *c.* 15 ka, the whole of the Aeron catchment and much of the Cambrian Mountains plateau were ice-free and the Teifi glacier had receded into the Tregaron area.

vi. A period of rapid deglaciation followed, which saw the Teifi glacier retreat into its upland source areas in the Cambrian Mountains prior to final down-wasting before the onset of the Windermere Interstadial around 13.5 ka. The deglaciation geochronology for south-west and south-central Wales matches that of parts of North Wales, confirming that the Welsh Ice Cap underwent a period of marked thinning and reconfiguration around 17–20 ka.

Abbreviations. BIIS, British–Irish Ice Sheet; CAM, central age model; DR, dose-recovery; DRAC, dose rate and age calculator; FMM, finite mixture model; HF, hydrofluoric; ICP-AES, inductively coupled plasma atomic emission spectroscopy; ICP-MS, inductively coupled plasma mass spectrometry; ISIS, Irish Sea Ice Stream; LGM, Last Glacial Maximum; MAM, minimum age model; OD, overdispersion; SUERC, Scottish Universities Environmental Research Centre; WIC, Welsh Ice Cap.

References

Aitken MJ, Alldred JC. 1972. The assessment of error limits in thermoluminescence dating. *Archaeometry* **14**: 257–267.

Balco G. 2011. Contributions and unrealized potential contributions of cosmogenic-nuclide exposure dating to glacier chronology, 1990–2010. *Quaternary Science Reviews* **30**: 3–27.

Balco G, Stone JO, Lifton NA *et al.* 2008. A complete and easily accessible means of calculating surface exposure ages or erosion rates from [10]Be and [26]Al measurements. *Quaternary Geochronology* **3**: 174–195.

Ballantyne CK. 2010. Extent and deglacial chronology of the last British–Irish Ice Sheet: implications of exposure dating using cosmogenic isotopes. *Journal of Quaternary Science* **25**: 515–534.

Ballantyne CK, Stone JO. 2012. Did large ice caps persist on low ground in north-west Scotland during the Lateglacial Interstade? *Journal of Quaternary Science* **27**: 297–306.

Björck S, Walker MJC, Cwynar LC *et al.* 1998. An event stratigraphy for the Last Termination in the North Atlantic region based on the Greenland ice-core record: a proposal by the INTIMATE group. *Journal of Quaternary Science* **13**: 283–292.

Blockley SPE, Bourne AJ, Brauer A *et al.* 2014. Tephrochronology and the extended intimate (integration of ice-core, marine and terrestrial records) event stratigraphy 8–128 ka b2k. *Quaternary Science Reviews* **106**: 88–100.

Bøtter-Jensen L, Andersen CE, Duller GAT *et al.* 2003. Developments in radiation, stimulation and observation facilities in luminescence measurements. *Radiation Measurements* **37**: 535–541.

Boulton GS, Jones AS, Clayton KM *et al.* 1977. A British ice-sheet model and patterns of glacial erosion and deposition in Britain. In *British Quaternary Studies: Recent Advances*, Shotton FW (ed.). Clarendon Press: Oxford; 231–246.

Boulton GS, Peacock JD, Sutherland DG. 1991. Quaternary. In *Geology of Scotland*, Craig GY (ed.). Geological Society: London; 503–543.

Boulton GS, Smith GD, Jones AS *et al.* 1985. Glacial geology and glaciology of the last mid-latitude ice sheets. *Journal of the Geological Society* **142**: 447–474.

British Geological Survey. 1989. *Aberystwyth. England and Wales Sheet 163. Drift Edition. 1: 50 000*. British Geological Survey: Keyworth.

British Geological Survey. 1993. *Rhayader. England and Wales Sheet 179. Drift Edition. 1:50 000*. British Geological Survey: Keyworth.

British Geological Survey. 1994. *Llanilar. England and Wales Sheet 178. Solid and Drift Geology. 1: 50 000*. British Geological Survey: Keyworth.

British Geological Survey. 2003. *Cardigan and Dinas Island. England and Wales Sheet 193. Solid and Drift Geology 1: 50 000*. British Geological Survey: Keyworth.

British Geological Survey. 2006a. *Aberaeron. England and Wales Sheet 177. Bedrock and Bedrock and Superficial Deposits. 1: 50 000*. British Geological Survey: Keyworth.

British Geological Survey. 2006b. *Llangranog. England and Wales Sheet 194. Bedrock and Superficial Deposits. 1: 50 000*. British Geological Survey: Keyworth.

British Geological Survey. 2007a. *Lampeter. England and Wales Sheet 195. Bedrock and Superficial Deposits. 1: 50 000*. British Geological Survey: Keyworth.

British Geological Survey. 2007b. *Newcastle Emlyn. England and Wales Sheet 211. Bedrock and Superficial Deposits. 1: 50 000*. British Geological Survey: Keyworth.

British Geological Survey. 2008. *Llandovery. England and Wales Sheet 212. Bedrock and Superficial Deposits. 1: 50 000*. British Geological Survey: Keyworth.

British Geological Survey. 2010. *Fishguard. England and Wales Sheet 210. Bedrock and Superficial Deposits. 1: 50 000*. British Geological Survey: Keyworth.

Burt CE, Aspden JA, Davies JR *et al.* 2012. *Geology of the Fishguard District: a Brief Explanation of the Geological Map. Sheet Explanation of the British Geological Survey, England and Wales Sheet 193*. British Geolgical Survey: Keyworth.

Charlesworth JK. 1929. The south Wales end-moraine. *Quarterly Journal of the Geological Society*, **85**: 335–358.

Child D, Elliott G, Mifsud C *et al.* 2000. Sample processing for earth science studies at ANTARES. *Nuclear Instruments and Methods in Physics Research Section B: Beam Interactions with Materials and Atoms* **172**: 856–860.

Chiverrell RC, Thrasher IM, Thomas GSP *et al.* 2013. Bayesian modelling the retreat of the Irish Sea Ice Stream. *Journal of Quaternary Science* **28**: 200–209.

Chmeleff J, von Blanckenburg F, Kossert K *et al.* 2010. Determination of the ^{10}Be half-life by multicollector ICP-MS and liquid scintillation counting. *Nuclear Instruments and Methods in Physics Research Section B: Beam Interactions with Materials and Atoms* **268**: 192–199.

Clark CD, Ely JC, Greenwood SL *et al.* 2018. BRITICE Glacial Map, version 2: a map and GIS database of glacial landforms of the last British-Irish Ice Sheet. *Boreas* **47**: 11.

Clark CD, Hughes ALC, Greenwood SL *et al.* 2012. Pattern and timing of retreat of the last British–Irish Ice Sheet. *Quaternary Science Reviews* **44**: 112–146.

Davies JR, Fletcher CJN, Waters RA, *et al.* 1997. *Geology of the country around Llanilar and Rhayader. Memoir of the British Geological Survey, Sheets 178 and 179 (England and Wales)*. British Geological Survey: Keyworth.

Davies JR, Schofield DI, Sheppard TH *et al.* 2006a. *Geology of the Lampeter District. Sheet Explanation of the British Geological Survey 1: 50 000 Sheet 195 Lampeter (England and Wales)*. British Geological Survey: Keyworth.

Davies JR, Sheppard TH, Waters RA *et al.* 2006b. *Geology of the Llangranog District: a Brief Explanation of the Geological Map. Sheet Explanation of the British Geological Survey, England and Wales Sheet 194*. British Geolgical Survey: Keyworth.

Davies JR, Waters RA, Wilby PR *et al.* 2003. *Geology of the Cardigan and Dinas Island District: a Brief Explanation of the Geological Map. Sheet Explanation of the British Geological Survey, England and Wales Sheet 193*. British Geolgical Survey: Keyworth.

Davies JR, Wilson D, Williamson IT. 2004 *Geology of the Country Around Flint. Memoir of the British Geological Survey, Sheet 108 (England and Wales)*. British Geological Survey: Keyworth.

Dunai TJ. 2010 *Cosmogenic Nuclides: Principles, Concepts and Applications in Earth Surface Sciences*. Cambridge University Press: Cambridge.

Durcan JA, King GE, Duller GAT. 2015. DRAC: Dose Rate and Age Calculator for trapped charge dating. *Quaternary Geochronology* **28**: 54–61.

Etienne JL, Hambrey MJ, Glasser NF *et al.* 2005. West Wales. In *The Glaciation of Wales and Adjacent Areas*, Lewis CA, Richards AE (eds). Logaston Press: Hereford; 85–100.

Etienne JL, Jansson KN, Glasser NF *et al.* 2006. Palaeoenvironmental interpretation of an ice-contact glacial lake succession: an example from the Late Devensian of southwest Wales, UK. *Quaternary Science Reviews* **25**: 739–762.

Everest JD, Bradwell T, Stoker MS *et al.* 2013. New age constraints for the maximum extent of the last British–Irish Ice Sheet (NW Sector). *Journal of Quaternary Science* **28**: 2–7.

Fearnsides WG. 1905. On the geology of Arenig Fawr and Moel Llyfnant. *Quarterly Journal of the Geological Society* **61**: 608–640.

Fletcher CJN, Siddle HJ. 1998. Development of glacial Llyn Teifi, west Wales: evidence for lake-level fluctuations at the margins of the Irish Sea ice sheet. *Journal of the Geological Society* **155**: 389–399.

Foster HD. 1970a. Sarn Badrig, a submarine moraine in Cardigan Bay, north Wales. *Zeitschrift für Geomorphologie* **14**: 473–486.

Foster HD. 1970b. Establishing the age and geomorphological significance of sorted stone-stripes in the Rhinog Mountains, North Wales. *Geografiska Annaler: Series A, Physical Geography* **52**: 96–102.

Glasser NF, Etienne JL, Hambrey MJ *et al.* 2004. Glacial meltwater erosion and sedimentation as evidence for multiple glaciations in west Wales. *Boreas* **33**: 224–237.

Glasser NF, Hughes PD, Fenton C *et al.* 2012. ^{10}Be and ^{26}Al exposure-age dating of bedrock surfaces on the Aran ridge, Wales: evidence for a thick Welsh Ice Cap at the Last Glacial Maximum. *Journal of Quaternary Science* **27**: 97–104.

Godwin H, Mitchell GF. 1938. Stratigraphy and development of two raised bogs near Tregaron, Cardiganshire. *New Phytologist* **37**: 425–454.

Golledge NR, Hubbard A, Sugden DE. 2008. High-resolution numerical simulation of Younger Dryas glaciation in Scotland. *Quaternary Science Reviews* **27**: 888–904.

Gosse JC, Phillips FM. 2001. Terrestrial *in situ* cosmogenic nuclides: theory and application. *Quaternary Science Reviews* **20**: 1475–1560.

Guerin G, Mercier N, Adamiec G. 2011. Dose-rate conversion factors: update. *Ancient TL* **29**: 5–8.

Guérin G, Mercier N, Nathan R *et al.* 2012. On the use of the infinite matrix assumption and associated concepts: a critical review. *Radiation Measurements* **47**: 778–785.

Hambrey MJ, Davies JR, Glasser NF *et al.* 2001. Devensian glacigenic sedimentation and landscape evolution in the Cardigan area of southwest Wales. *Journal of Quaternary Science* **16**: 455–482.

Hibbert FA, Switsur VR. 1976. Radiocarbon dating of Flandrian pollen zones in Wales and northern England. *New Phytologist* **77**: 793–807.

Hubbard AL, Bradwell T, Golledge N *et al.* 2009. Dynamic cycles, ice streams and their impact on the extent, chronology and deglaciation of the British–Irish ice sheet. *Quaternary Science Reviews* **28**: 758–776.

Hubbard BP, Glasser NF. 2006. Field Techniques in Glaciology and Glacial Geomorphology. *John Wiley and Sons: Hoboken.*

Hughes ALC, Clark CD, Jordan CJ. 2014. Flow-pattern evolution of the last British Ice Sheet. *Quaternary Science Reviews* **89**: 148–168.

Hughes ALC, Greenwood SL, Clark CD. 2011. Dating constraints on the last British–Irish Ice Sheet: a map and database. *Journal of Maps* **7**: 156–184.

Hughes PD, Glasser NF, Fink D. 2016. Rapid thinning of the Welsh Ice Cap at 20–19 ka based on ^{10}Be ages. *Quaternary Research* **85**: 107–117.

Jansson KN, Glasser NF. 2005. Palaeoglaciology of the Welsh sector of the British–Irish Ice Sheet. *Journal of the Geological Society* **162**: 25–37.

Jenkins GTH, Duller GAT, Roberts HM *et al.* 2018. A new approach for luminescence dating glaciofluvial deposits − high precision optical dating of cobbles. *Quaternary Science Reviews* **192**: 263–273.

Jones OT. 1965. The glacial and post-glacial history of the lower Teifi valley. *Quarterly Journal of the Geological Society* **121**: 247–281.

Korschinek G, Bergmaier A, Faestermann T *et al.* 2010. A new value for the half-life of ^{10}Be by heavy-ion elastic recoil detection and liquid scintillation counting. *Nuclear Instruments and Methods in Physics Research Section B: Beam Interactions with Materials and Atoms* **268**: 187–191.

Lal D. 1991. Cosmic ray labeling of erosion surfaces: in situ nuclide production rates and erosion models. *Earth and Planetary Science Letters* **104**: 424–439.

Lambeck K. 1993. Glacial rebound of the British Isles. II. A high-resolution, high-precision model. *Geophysical Journal International* **115**: 960–990.

Lambeck K. 1995. Late Devensian and Holocene shorelines of the British Isles and North Sea from models of glacio-hydro-isostatic rebound. *Journal of the Geological Society* **152**: 437–448.

McCarroll D, Ballantyne CK. 2000. The last ice sheet in Snowdonia. *Journal of Quaternary Science* **15**: 765–778.

McCarroll D, Stone JO, Ballantyne CK *et al.* 2010. Exposure-age constraints on the extent, timing and rate of retreat of the last Irish Sea Ice Stream. *Quaternary Science Reviews* **29**: 1844–1852.

McMillan AA, Powell JH. 1999. *The Classification of Artificial (Man Made) Ground and Natural Superficial Deposits. British Geological Survey Research Report, RR/99/04.*

Merrin PD. 1999. *Report on the drilling and installation of exploratory boreholes, Afon Teifi Valley, west Wales. Report of the British Geological Survey, WD/99/24.*

Murray AS, Wintle AG. 2000. Luminescence dating of quartz using an improved single-aliquot regenerative-dose protocol. *Radiation Measurements* **32**: 57–73.

Nishiizumi K. 2004. Preparation of ^{26}Al AMS standards. *Nuclear Instruments and Methods in Physics Research Section B: Beam Interactions with Materials and Atoms* **223**: 388–392.

Nishiizumi K, Imamura M, Caffee MW *et al.* 2007. Absolute calibration of ^{10}Be AMS standards. *Nuclear Instruments and Methods in Physics Research Section B: Beam Interactions with Materials and Atoms* **258**(2): 403–413.

Owen G. 1997. Origin of an esker-like ridge − erosion or channel-fill? Sedimentology of the Monington 'Esker' in southwest Wales. *Quaternary Science Reviews* **16**: 675–684.

Patton H, Hambrey MJ. 2009. Ice-marginal sedimentation associated with the Late Devensian Welsh Ice Cap and the Irish Sea Ice Stream: Tonfanau, West Wales. *Proceedings of the Geologists' Association* **120**: 256–274.

Patton H, Hubbard A, Glasser NF *et al.* 2013a. The last Welsh Ice Cap: Part 1 − Modelling its evolution, sensitivity and associated climate. *Boreas* **42**: 471–490.

Patton H, Hubbard A, Glasser NF *et al.* 2013b. The last Welsh Ice Cap: Part 2 - Dynamics of a topographically controlled icecap. *Boreas* **42**: 491–510 [DOI: 10.1111/j.1502-3885.2012.00301.x].

Patton H, Hubbard A, Bradwell T *et al.* 2013c. Rapid marine deglaciation: asynchronous retreat dynamics between the Irish Sea Ice Stream and terrestrial outlet glaciers. *Earth Surface Dynamics* **1**: 53–65.

Peltier WR, Fairbanks RG. 2006. Global glacial ice volume and Last Glacial Maximum duration from an extended Barbados sea level record. *Quaternary Science Reviews* **25**: 3322–3337.

Phillips FM, Bowen DQ, Elmore D. 1994. Surface exposure dating of glacial features in Great Britain using cosmogenic Chlorine-36: preliminary results. *Mineralogical Magazine* **58a**: 722–723.

Prescott JR, Hutton JT. 1994. Cosmic ray contributions to dose rates for luminescence and ESR dating: large depths and long-term time variations. *Radiation Measurements* **23**: 497–500.

Ross N. 2006. *Re-evaluation of the origins of Late Quaternary ramparted depressions in Wales.* PhD Thesis, Cardiff University.

Rowlands BM. 1971. Radiocarbon evidence of the age of an Irish Sea Glaciation in the vale of Clwyd. *Nature Physical Science* **230**: 9–11.

Sahlin EA. 2010. *Palaeoglaciology and geomorphology of the Central and Northern Cambrian Mountains, Wales.* PhD Thesis, University of Wales, Aberystwyth.

Sahlin EA, Glasser NF, Rowlands AP. 2007. Geomorphological mapping in Wales, UK, based on remotely sensed data. *Grazer Schriften der Geographie und Raumforschung* **43**: 67–70.

Scourse JD, Haapaniemi AI, Colmenero-Hidalgo E *et al.* 2009. Growth, dynamics and deglaciation of the last British–Irish ice sheet: the deep-sea ice-rafted detritus record. *Quaternary Science Reviews* **28**: 3066–3084.

Smedley RK, Scourse JD, Small D *et al.* 2017a. New age constraints for the limit of the British–Irish Ice Sheet on the Isles of Scilly. *Journal of Quaternary Science* **32**: 48–62.

Smedley RK, Chiverrell RC, Burke MJ *et al.* 2017b. Internal dynamics condition millennial-scale oscillations of a retreating ice stream margin. *Geology* **49**: 787–790.

Stone JO. 2000. Air pressure and cosmogenic isotope production. *Journal of Geophysical Research: Solid Earth* **105**: 23753–23759.

Thomas GSP. 1985. The late-Devensian glaciation along the border of northest Wales. *Geological Journal* **20**: 319–340.

Thomas GSP. 1989. The Late Devensian glaciation along the western margin of the Cheshire–Shropshire lowland. *Journal of Quaternary Science* **4**: 167–181.

Thomas GSP, Chiverrell RC. 2007. Structural and depositional evidence for repeated ice-marginal oscillation along the eastern margin of the Late Devensian Irish Sea Ice Stream. *Quaternary Science Reviews* **26**: 2375–2405.

Thomsen KJ, Murray AS, Bøtter-Jensen L. 2005. Sources of variability in OSL dose measurements using single grains of quartz. *Radiation Measurements* **39**: 47–61.

Travis CB. 1944. The glacial history of the Berwyn hills, North Wales. *Proceedings of the Liverpool Geological Society* **19**: 14–28.

Walker MJC, Buckley SL, Casedine AE. 2001. Landscape change and human impact in west Wales during the Lateglacial and Flandrian. In *The Quaternary of West Wales: Field Guide*, Walker MJC, McCarroll (eds). Quaternary Research Association: London; 17–29.

Waters RA, Davies JR, Wilson D *et al.* 1997. A geological background for planning and development in the Afon Teifi catchment. *British Geological Survey Technical Report WA/97/35.*

Watson E. 1965. Periglacial structures in the Aberystwyth region of central Wales. *Proceedings of the Geologists' Association* **76**: 443–462.

Watson E. 1969. The periglacial landscape of the Aberystwyth region. In *Geography at Aberystwyth*, Bowen EG, Carter H, Taylor JA (eds). University of Wales Press: Cardiff; 35–49.

Wilby PR, Schofield DI, Wilson D *et al.* 2007. *Geology of the Newcastle Emlyn District: a Brief Explanation of the Geological Map. Sheet Explanation of the British Geological Survey, England and Wales Sheet 211.* British Geological Survey: Keyworth.

Xu S, Dougans AB, Freeman S *et al.* 2010. Improved Be-10 and Al-26 AMS with a 5 MV spectrometer. *Nuclear Instruments and Methods in Physics Research, Section B: Beam Interactions with Materials and Atoms* **268**: 737–738.